

Research of the stress-strain state of rods obtained by porous blank extrusion

Cite as: AIP Conference Proceedings **1915**, 030003 (2017); <https://doi.org/10.1063/1.5017323>
Published Online: 12 December 2017

I. M. Berezin, A. P. Polyakov, and P. A. Polyakov



View Online



Export Citation

ARTICLES YOU MAY BE INTERESTED IN

Waves of pressure in viscous incompressible fluid

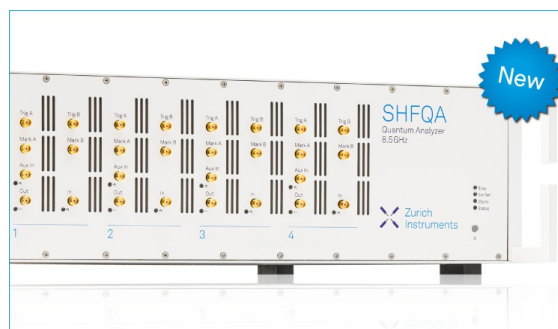
AIP Conference Proceedings **1915**, 020006 (2017); <https://doi.org/10.1063/1.5017318>

Effect of strain rate on the formation of the microstructure of a 1950/10% SiC metal matrix composite under high temperature

AIP Conference Proceedings **1915**, 030002 (2017); <https://doi.org/10.1063/1.5017322>

Studying damage accumulation in martensitic corrosion-resistant steel under cold radial reduction

AIP Conference Proceedings **1915**, 030007 (2017); <https://doi.org/10.1063/1.5017327>



Your Qubits. Measured.

Meet the next generation of quantum analyzers

- Readout for up to 64 qubits
- Operation at up to 8.5 GHz, mixer-calibration-free
- Signal optimization with minimal latency

Find out more

 Zurich Instruments

Research of the Stress-Strain State of Rods Obtained by Porous Blank Extrusion

I. M. Berezin^{1, 2, a)}, A. P. Polyakov^{1, b)} and P. A. Polyakov^{1, c)}

¹*Institute of Engineering Science, Ural Branch of the Russian Academy of Sciences,
34 Komsomolskaya St., Ekaterinburg, 620049, Russia, Tel.: (343) 375-35-90*

²*B. N. Yeltsin Ural Federal University, 19 Mira St., Ekaterinburg, 620002, Russia*

^{a)}Corresponding author: berezin@imach.uran.ru

^{b)}pap@imach.uran.ru

^{c)}pavel.katsu@gmail.com

Abstract. The features of the stress-strain state in the cross section of rods under forming are revealed by the finite element modeling of the process of direct extrusion of a porous iron blank. In particular, the nature of porosity distribution and the stress-state stiffness coefficient obtained as a result of calculating the residual stresses field in the rod is studied. The Gurson-Tvergaard-Needleman (GTN) model is used to describe the behavior of the material of a porous blank under plastic deformation. It has been established that, in different cross-section zones of the rod, the values of the stress-state coefficient can be either positive or negative. It is shown that the most unfavorable area of the cross-section in the drawing index range investigated (2.04-4) is the material layer lying in the immediate vicinity of the outer surface of the rod (0.7...0.8R, where R is the rod radius), where the localization of tensile stresses is observed which promotes the emergence and growth of layered annular cracks.

INTRODUCTION

Extrusion is one of the main technological processes of powder metallurgy. Large plastic deformations arising during extrusion contribute to the effective closure of pores and have a positive effect on the formation of the extruded blank structure [1]. It is known that plastic deformations are accompanied by a gradual accumulation of submicroscopic discontinuities and their development. In this case, after extrusion, significant residual stresses are generated in the piece, which may cause the development of submicroscopic and microscopic cracks and the appearance of macrodefects (Fig. 1a). The analytical models of the process make it possible to determine the extrusion force and the residual porosity of the rods. Predicting the appearance of various kinds of defects resulting from the influence of the shape of the deforming tool, the drawing index, the contact friction conditions and other factors is a complex task that requires the use of numerical methods, in particular, the finite element method. The aim of this work is to study the stress-strain state of rods after unloading based on computer simulation of the process of direct extrusion of porous blanks in order to determine the location of defects and explain the causes of their probable occurrence.

NUMERICAL MODELING

For the complex stress-strain state of bodies with structural defects (pores), models taking into account both compaction and decompaction, such as the Cam-Clay Plasticity model [2], the Gurson-Tvergaard-Needleman model [3, 4], the Modified Drucker-Prager Cap model [5], used in finite element analysis, are the most appropriate ones. A number of models work well in high-density areas, but underestimate the results in low-density ones, and vice versa [6]. In particular, the Gurson model generally gives physically reasonable results only for a sufficiently high relative

material density, usually $\rho_{\text{rel}} \geq 0.9$ [7]. The model allows taking into account the change in volume void fraction (VVF) during plastic deformation, caused by the growth of existing pores and the appearance of new ones.

The yield criterion is expressed as

$$\Phi = \left(\frac{q}{\sigma_y} \right)^2 + 2q_1 \cdot f \cdot \cosh \left(-q_2 \frac{3p}{2\sigma_y} \right) - (1 + q_3 f^2) = 0, \quad (1)$$

where q is the effective Mises stress; p is the hydrostatic pressure; $p = -\sigma$, where σ is the hydrostatic stress; σ_y is the yield stress of the fully dense material; and q_1, q_2, q_3 are material parameters. The original Gurson model is recovered when $q_1 = q_2 = q_3 = 1.0$. For typical metals, the ranges of the parameters q_1, q_2, q_3 reported in the literature are $q_1 = 1.0$ to 1.5 , $q_2 = 1.0$, and $q_3 = q_1^2 = 1.0$ to 2.25 [3]. It should be noted that these values of the coefficients adequately describe the behavior of the material under deformation schemes with prevailing tensile stresses. Since a different stress-strain scheme is implemented during extrusion, in particular, that characterized by considerable deformations of all-round compression and shear, the values of the parameters q_1, q_2, q_3 were chosen on the basis of the correspondence between the calculated and experimental data. In particular, in case of using the coefficients $q_1, q_2, q_3 > 1$ during modeling, the extruded rods reached their 100% density even upon the drawing index $\mu = (D_1)^2/(D_2)^2 = 3$ (where D_1 is the initial diameter of the blank, D_2 is the diameter of the rod after extrusion), and this contradicts the numerous theoretical and experimental data. It is known that the production of quasimonolithic rods from powdered and porous metallic materials by direct extrusion through a conical die is achieved at best upon the drawing index $\mu > 6$. As a result, it was assumed for calculations that $q_1 = 0.5, q_2 = 0.5, q_3 = q_1^2 = 0.25$.

The problem was solved in an axisymmetric formulation. Computer simulation was carried out by the finite element method in Abaqus/Standard. The CAX4R uniform grid of four-node finite elements was used; their total number was 1000. The material is described by an elastoplastic model: modulus of elasticity $E = 190$ GPa, Poisson's ratio $\nu = 0.27$. The yield point of a non-porous material (perfect plasticity) is $q = 433$ MPa. The value is obtained on the basis of an analytical calculation of the energy-force parameters of the extrusion of iron-based powder blanks and identification of calculated dependences from the experimental results. When choosing the friction conditions between the porous billet and the compression mold, the data of [8] are used, which shows the results of an investigation of the tribological characteristics of iron-based powder blanks. The Siebel friction law is used with the friction coefficient $\psi = 0.3$. The calculations were performed with the initial diameter of the blank 10 mm and the drawing index $\mu = 2.04, 2.78$ and 4 . The initial relative density was assumed as equal to $\rho_{\text{rel}} = 0.88$. The die cone angle α is 30° .

RESULTS AND DISCUSSION

The simulation results are shown in Fig. 1–3. The maximum value of the effective stresses by Mises q (Fig. 1, a) and hydrostatic stresses σ (Fig. 1, b) is reached inside the deformation zone. It can be seen that the compaction process is concentrated in the range of the combination of the maximum shear and hydrostatic deformation values (Fig. 1, c). After the rod leaves the die calibration band, the stress in the material is relaxed. At the same time, for all the considered drawing values, along the blank axis ($\lambda = r/R = 0$, where r is the distance from the rod axis to the zone of the measurement of the stress-strain state parameters, R is the radius of the rod), negative average normal stresses σ prevail, decreasing with an increase in the drawing index μ . The effective Mises stresses on the rod axis also decrease as the drawing value increases. On the rod periphery, a soft stress state scheme predominates ($\sigma < 0$), while localization of tensile stresses ($\sigma > 0$) is observed in material layers close to the outer surface of the rods ($\lambda = 0.7 \dots 0.8$). The distribution of porosity in the rod cross section is also extremely uneven; the porosity decreases from the axis of the rod symmetry to its periphery, while the degree of unevenness decreases as the drawing increases.

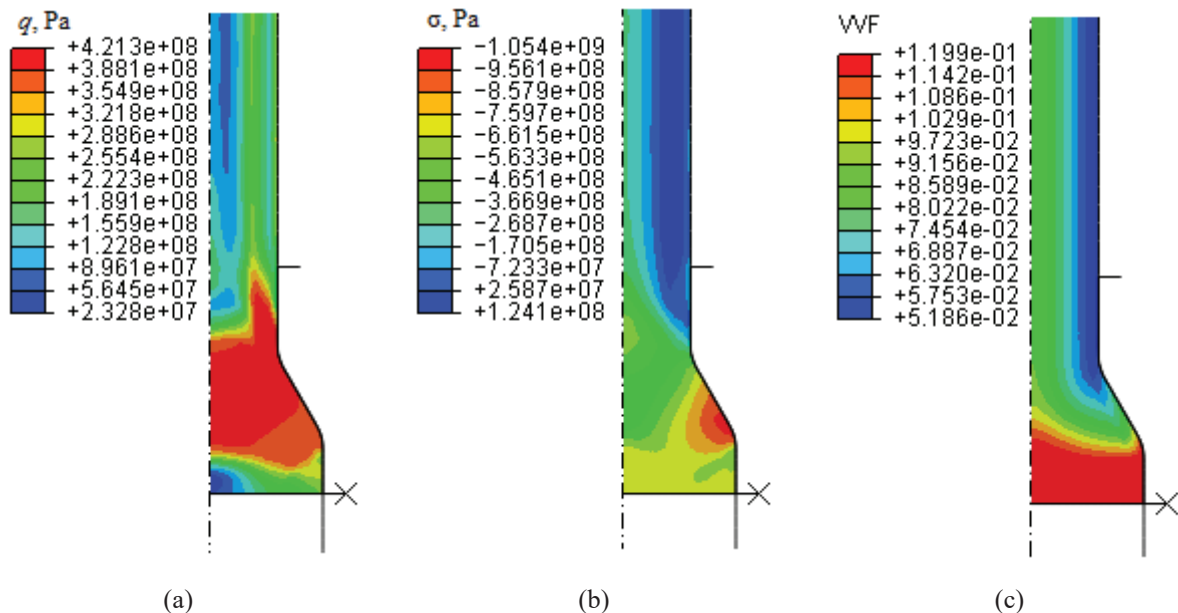


FIGURE 1. Distribution of effective Mises stress (a), hydrostatic stress (b) and volume void fraction (c) in the 1/2 axial section of the extruded rod upon the drawing index $\mu = 2.78$

Figure 2 shows a diagram of the change in the extrusion force from the displacement of the punch for the drawing index $\mu = 2.04$. It can be seen that the process of direct extrusion is divided into two main stages by changes in the force and deformation conditions. During the initial stage of the process (I), the blank is pressed out in the container, and the material of the conical die channel is filled with the extruded material. The second stage of the process (II) is characterized by a steady metal flow. The nature of the curve obtained by computer simulation qualitatively coincides with the experimental results. After reaching the maximum value of the extrusion force, the falling branch of the calculated curve lies above the experimental curve, and this may be due to more complicated conditions of interaction between the blank material and the pressing equipment.

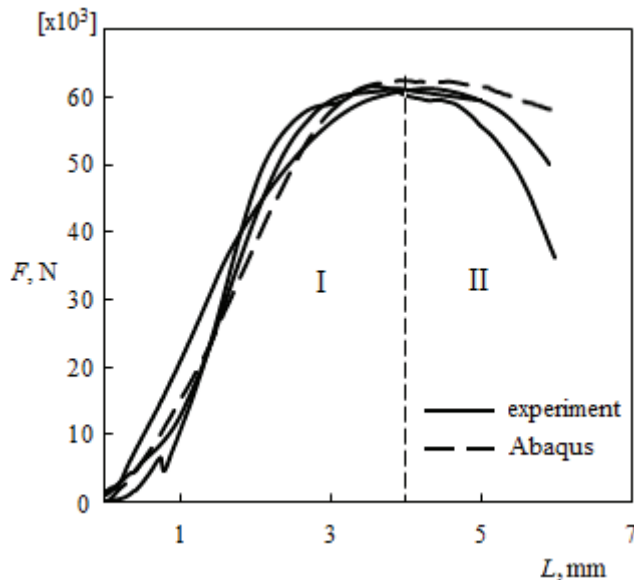


FIGURE 2. Dependence of the extrusion force on punch displacement

Figure 3 shows the nature of the distribution of the residual volume void fraction (porosity) and the value of the stress-state coefficient $k = \sigma/\tau$ (σ is hydrostatic stress, τ is the intensity of shear stress).

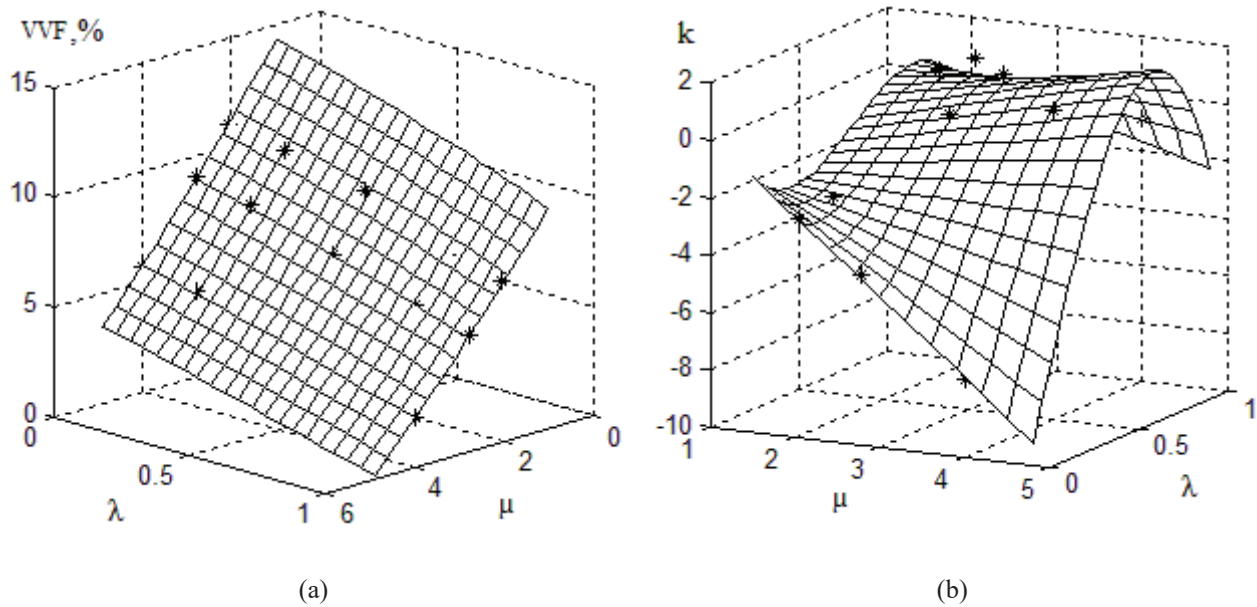


FIGURE 3. The distribution of the volume void fraction (a) and the stiffness coefficient of the stressed state k (b) as a function of the drawing index μ and the parameter λ

CONCLUSIONS

1. It has been demonstrated that, in different cross-section zones of the rod, the values of the stress-state coefficient can be either positive (rigid stress-state scheme) or negative (soft stress-state scheme). The unevenness of the stress state over the rod cross section increases with drawing. At the periphery of the extruded rods, when the drawing is changed, the value of the stress-state coefficient remains practically unchanged, while on the blank axis the coefficient k changes more than by a factor of 3.

2. It has been established that, in the layers of the material close to the outer surface of the rods ($0.7...0.8R$, where R is the rod radius), the localization of tensile stresses is observed, whereas on the outer surface of the rods and on the rotation axis, a soft stress state scheme $k < 0$ predominates.

3. The process of direct extrusion of porous blanks has significant disadvantages, which predetermine the production of defects both on the surface and in the inner part of the rods. On the one hand, the central part of the rod is the least dense and contains a large number of pores and defects. On the other hand, in the layers of the material lying in the immediate vicinity ($0.7...0.8R$) of the outer surface of the extruded rods, considerable tensile stresses exist in the drawing range, which may contribute to the occurrence and development of annular cracks.

REFERENCES

1. G. Sjöberg, V. Mironov, H. E Fischmeister, *Powder Metallurgy Int.* **9**, 160–163 (1977).
2. A. Schofield and C. P. Wroth, *Critical State Soil Mechanics* (McGraw-Hill, New York, 1968), p. 218.
3. A. L. Gurson, *Journal of Engineering Materials and Technology* **99**, 2–15 (1977).
4. V. Tvergaard, A. Needleman, *Acta Metallurgica* **32**, 157–169 (1984).
5. L. Resende, J. B. Martin, *Journal of Engineering Mechanics* **111**, 855–881 (1985).
6. S. C. Lee, K. T. Kim, *International Journal of Mechanical Sciences* **44**, 1295–1308 (2002).
7. ABAQUS 6.10 Theory Manual. Providence, United States: Dassault Systemes Simulia Corp (2010).
8. S. N. Grigoriev, A. N. Krasnovskii, *Journal of Friction and Wear* **32**, 164–166 (2011).